

# Implementation of Inverted-Pair EMI Detector on the Monte-Carlo Based Simulation Frameworks

Hasan Habib  
M-Group  
KU Leuven Bruges Campus  
8200 Bruges, Belgium  
hasan.habib@kuleuven.be

Tim Claeys  
M-Group  
KU Leuven Bruges Campus  
8200 Bruges, Belgium  
tim.claeys@kuleuven.be

Jonas Lannoo  
M-Group  
KU Leuven Bruges Campus  
8200 Bruges, Belgium  
jonas.lannoo@kuleuven.be

Dries Vanoost  
M-Group  
KU Leuven Bruges Campus  
8200 Bruges, Belgium  
dries.vanoost@kuleuven.be

Guy A. E. Vandenbosch  
ESAT-Telemic  
KU Leuven  
3001 Leuven, Belgium  
guy.vandenbosch@kuleuven.be

Davy Pissoort  
M-Group  
KU Leuven Bruges Campus  
8200 Bruges, Belgium  
davy.pissoort@kuleuven.be

**Abstract**—The goal of this paper is to implement the design of a previously proposed inverted-pair EMI detector on the Monte-Carlo based simulation framework. The inverted-pair EMI detector can detect electromagnetic disturbances in the wired communication channel, and generate a warning. The warning generated by the detector helps the system to follow the precautionary procedure, including safe-state operation or re-transmission of data. In order to verify the theoretical results, the performance of EMI detector is evaluated in real-like reverberation environment using the simulation framework. The simulation framework uses efficient reciprocity-based algorithm to find out voltages and currents induced due to Electro-magnetic (EM) waves; these induced voltages and currents add up with the transmitted signal in data transmission lines, disturbing the actual data. The inverted-pair EMI detector aims to identify these disturbances in the reverberation room environment, thereby performing similar to previously analysed theoretical results.

**Index Terms**—EMI Sensors, EMI Risk management, EMC, functional safety, simulation-framework

## I. INTRODUCTION

As we are moving toward advance technologies, including smart cities, Internet-of-Things(IoT), autonomous vehicles and industry 4.0, our lives are more and more connected with a number of electronic devices. Although technology is continuously adding comfort to our lives, at the same speed, concerns related safety of electronic devices is gaining significant importance, especially for safety- and mission-critical systems [1]. All Electrical/Electronic devices generate some un-intentional EM waves, and at the same time, in terms of safety, these devices are also sensitive to Electromagnetic Interference (EMI). EMI can corrupt the data, and in extreme cases, cause fatal errors. As we are moving toward more hi-tech systems, all electronic devices are facing harsh electro-

magnetic environment [2]. For the same reason, EMI Risk Management has received significant attention in the recent past, leading to the generation of several standards and guides for the Functional Safety of the system considering aspects of Electro-Magnetic Compatibility (EMC) [3].

Unfortunately, most of the Techniques and Measures (T&Ms) developed by researchers focuses on safe data transmission or correction of data. These T&Ms include following hardware-based techniques of using time, frequency and spatial diversity along with redundancy and software-based techniques including Error Detection and Error Correction Codes (EDC/ECC). Apart from the risk factor of fatal error because of failure of these T&Ms, they also result in significant processing delay, heavy cost of computation and transmission of extra data [4], [5].

The aim of our research is to analyse the performance of an inverted-Pair EMI detector proposed in the ..... paper in the reverberation room environment. Inverted-Pair EMI detector aims to generate a warning when EMI disturbs the data transmitted on the data transmission lines. This warning can help the system to initiate the precautionary procedure that will help to reduce the risk of fatal errors due to EMI. Initially, results of the detector are analysed using the theoretical simulations, using the continuous sinewave signal as EMI induced voltage source at a different frequency, amplitude and phase. Theoretical results of Inverted-Pair EMI detector shows that it can detect EMI for all cases except when frequency ratio is integer multiple of number of samples per bit and phase difference between EMI induced voltage at both data transmission lines is quite large, where frequency ratio is defined as ratio of EMI frequency  $f_{EMI}$  to bit frequency  $f_{BIT}$  given in (1).

$$f_{ratio} = \frac{f_{EMI}}{f_{BIT}} \quad (1)$$

In the real-like environment, randomly distributed electronic devices generate arbitrary EM waves, resembling the en-

The research leading to these results has received funding from the European Union's Horizon 2020 research and innovation programme under the Marie Skłodowska-Curie Grant Agreement No 812.790 (MSCA-ETN PETER). This publication reflects only the authors' view, exempting the European Union from any liability. Project website: <http://etn-peter.eu/>.

environment of reverberation room. Simulation-framework is employed to verify the performance of EMI detector in real-like reverb-environment. Simulation framework facilitates the creation of a mathematical model for random EM waves and their induced voltages and currents, also to analyse the performance of the EMI detector.

The remainder of this paper is organized as follows: Section II briefly describes the Geometry of the system under study. Section III shows calculation of induced voltages and currents in reverberation room environment. Section IV represents basics of inverted-pair EMI detector. Section V deduces the outcome from the results and section VI draws a conclusion.

## II. GEOMETRY UNDER STUDY

Two 50 ohms microstrips, as shown in Fig. 1 with identical shapes are extracted on FR4 substrate of 10cm by 16cm, thickness of a substrate is 1.6mm. These microstrips are used as data line and inverted data line, both data transmission lines are driven by 1V power supply, they have 50 Ohm output impedance, and they are terminated with 50 Ohm load. The space between both data transmission lines is fixed at 10 mm (centre to centre) in the start and then stepwise increased.

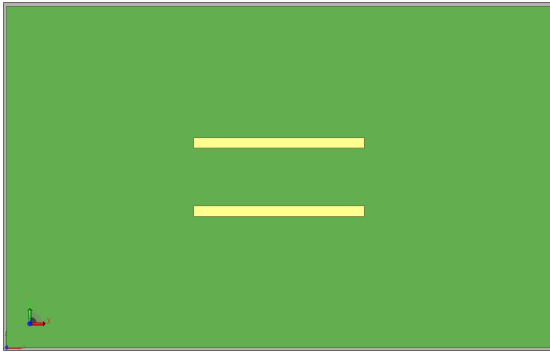


Fig. 1: Data transmission line on the substrate, distance between data transmission lines (centre to centre) = 10 mm

## III. CALCULATION OF INDUCED VOLTAGES IN REVERBERATION ROOM ENVIRONMENT

As real-world EM environment consists of a number of plane waves and their reflections, this is obtained in simulation-framework by superposition of statically distributed random plane waves. A number of plane waves practically show a number of sources that are simultaneously excited in the real reverberation chamber. Reciprocity-based efficient algorithm is used to determine the worst-case induced voltages and currents generated by random incident plane waves in Multiconductor-Transmission-Line (MTL). This algorithm determines the behaviour of antenna in a receive mode by using the induced voltages and currents at the antenna ports/microstrip in the transmit mode. Using the method given in [6], this algorithm allows calculation of induced voltages and currents by using one full wave simulation per excited port rather than separate simulation for each EM disturbance. The induced voltage in each data transmission line while

transmitting a particular signal is a sum of voltages induced by all plane waves at a specific instant. As total power by plane waves in this case is more than actual power, therefore normalisation rule is applied for the separate plane wave as given in (2).

$$E_N = \frac{E_o}{N} \quad (2)$$

N is a total number of plane waves, for the simulations below N is chosen as 200. Properties of each plane waves including polar angle, azimuth angle, polarisation angle and phase angle are chosen completely random for each simulation. In order to present uninterrupted reverberant environment simulations are performed M number of time, with randomly chosen properties of plane waves. For all of the analysis below M=1000.

## IV. INVERTED PAIR EMI DETECTOR

Proposed EMI detector is used for the detection of unwanted electromagnetic disturbances on the wired communication channel. Inverted-Pair EMI detector uses two data transmission lines. One data transmission line transmits the normal data while other data transmission line is used for transmitting inverted data. Data transmission lines use unipolar Non-Return-to-Zero-Level (NRZ-L) encoding, where 1V represents the binary '1', and 0V represents binary '0'. Data transmission lines continuously transmit data using pre-determined time for the transmission of each bit, and bits are transmitted with the frequency of  $f_{BIT}$ . Receiver samples the data in the mid and interprets voltage more than 0.66V as '1' and lower than 0.33V as '0'. Fig. 2 shows the block diagram of the inverted-pair EMI detector.

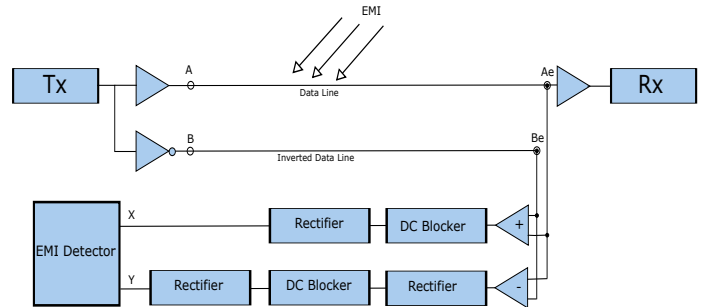


Fig. 2: EMI Detector Block Diagram

To detect EMI disturbance efficiently, EMI detector uses additional hardware. EMI detector samples multiple sample per bit  $f_{Samples}$ . For the simulations given below  $f_{Samples} = 3$  is chosen, as there was not significant improvement in results by a further increase and infinite  $f_{Samples}$  is not possible because of hardware limitation. Main goal of the hardware used by EMI detector is to create the following signals. As sampling at edges is prone to switching noise, samples are sampled at equally divided intervals as shown in Fig. 3

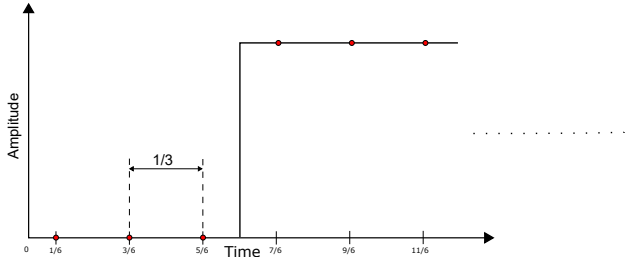


Fig. 3: Sampling of the Bits

In case, signal  $A(t)$  and  $B(t)$  are transmitted from the data and inverted data lines,  $EMI(t)$  and  $EMI_i(t)$  represents EMI induced voltage added to these lines. The main goal of the hardware used by EMI detector is to create the following signals.

$$X = |(A_e + B_e) - \text{mean}(A_e + B_e)| \quad (3)$$

$$Y = ||A_e - B_e| - \text{mean}|A_e - B_e||. \quad (4)$$

where

$$A_e(t) = A(t) + EMI(t) \quad (5)$$

$$B_e(t) = B(t) + EMI_i(t) \quad (6)$$

(3) helps to calculate the sum of EMI disturbance in both lines by using the multiple samples per bit. Initially, the EMI detector adds the signal from both data transmission lines followed by removal of DC voltage and rectification. When the phase difference between two lines is zero, ideally (3) should detect all EMI disturbance and generate a warning. As data transmission lines are not identically at the same place, there is a small distance between them. For the same reason, EM disturbance experiences the phase difference between both data transmission line. In the case of large phase difference, (3) is unable to detect all EMI disturbances. (4) calculates the difference of EMI induced voltages in both data transmission lines. Signal from both data transmission lines is subtracted, followed by rectification, removal of dc component and rectification again. EMI detector generates the warning if maxima all samples per bit of either (3) or (4) or both are more than a threshold voltage, defined as  $V_{\text{thres}}$ .

## V. EVALUATING THE EMI DETECTOR

In order to verify the performance of EMI detector in a reverberation room environment, 100 random bits are transmitted using the data transmission line using the simulation framework. Data line transmits the normal data while an inverted-data line transmits the same data in inverted form. In case the data line is transmitting 0, the inverted-data line will transmit 1 or vice-versa. Both data transmission lines are disturbed by EMI induced voltage by 200 random plane waves. For each transmitted bit, incident electric field  $E_{\text{inc}}$  varies from 1 V/m to  $10^9$  V/m and for each value of  $E_{\text{inc}}$  simulations are repeated 1000 times to get a clear idea of induced voltages in the data transmission lines.

The EMI detector should ideally detect all bit errors because of EMI in the data transmission lines and generate the warning. Still, there are cases when EMI detector fails to detect bit errors because of EMI; known as false negatives. Also, there are cases when EMI detector generates the warning while EMI is not disturbing the transmitted data; known as false positives. BER, false negative, false positives and warnings shown in this section are in percentage term. As it is very difficult to analyse the performance of EMI detector for the different voltage encoding with varying values of EMI induced voltage, SIR is defined. SIR is a ratio between the root mean square (rms) of the transmitted signal  $A_{\text{rms}}$  divided by the rms of the EMI induced voltage  $EMI_{\text{rms}}$  as given in (7).

$$SIR = 20 \cdot \log_{10} \left( \frac{A_{\text{rms}}}{EMI_{\text{rms}}} \right). \quad (7)$$

Fig. 4 shows the performance of EMI detector when data transmission lines are transmitting data at 500 MHz and simultaneously exposed to EMI disturbance of 500 MHz. Figure below shows EMI detector is able to detect all bit errors because of EMI i.e. no false negatives. Although there are cases when EMI detector generates a warning, but EMI is not disturbing the transmitted data, i.e. false positives.

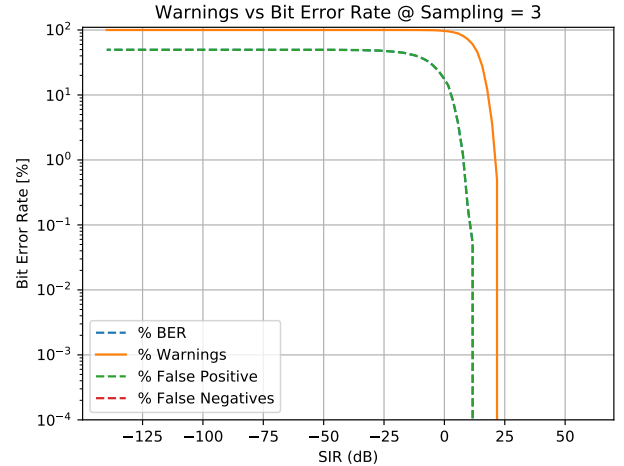


Fig. 4: Response of the EMI Detector for  $f_{\text{ratio}} = 1$  i.e.  $f_{\text{BIT}} = 500\text{MHz}$ ,  $f_{\text{EMI}} = 500\text{MHz}$ , distance between data transmission lines = 10mm

Fig. 5, Fig. 6, Fig. 7 and Fig. 8 shows response of EMI detector when  $f_{\text{ratio}}$  is multiple of sampling i.e. data is transmitted at 166.666666MHz while EMI of 500MHz disturbs the transmitted signal. Distance between both data transmissions lines is varied for each simulation. At the same frequency of EMI, an increase in distance between data transmission lines, raises the phase difference of EMI induced voltages in both lines. Figures show as distance between data transmission line is increased, EMI detector generates more false negatives.

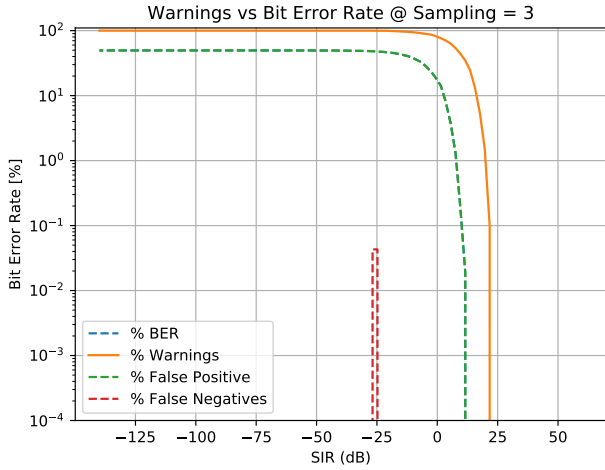


Fig. 5: Response of the EMI Detector for  $f_{\text{ratio}} = 3$  i.e.  $f_{\text{BIT}} = 166\text{MHz}$ ,  $f_{\text{EMI}} = 500\text{MHz}$ , distance between lines = 10mm

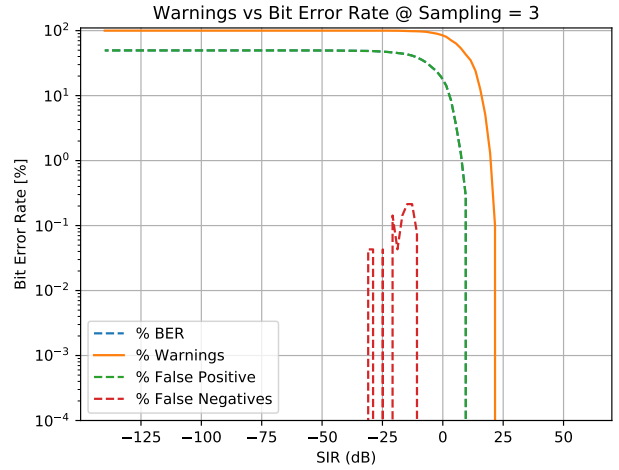


Fig. 7: Response of the EMI Detector for  $f_{\text{ratio}} = 3$  i.e.  $f_{\text{BIT}} = 166\text{MHz}$ ,  $f_{\text{EMI}} = 500\text{MHz}$ , distance between lines = 40mm

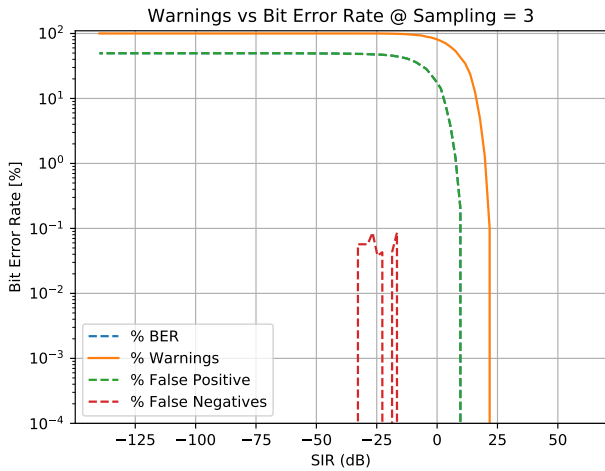


Fig. 6: Response of the EMI Detector for  $f_{\text{ratio}} = 3$  i.e.  $f_{\text{BIT}} = 166\text{MHz}$ ,  $f_{\text{EMI}} = 500\text{MHz}$ , distance between lines = 20mm

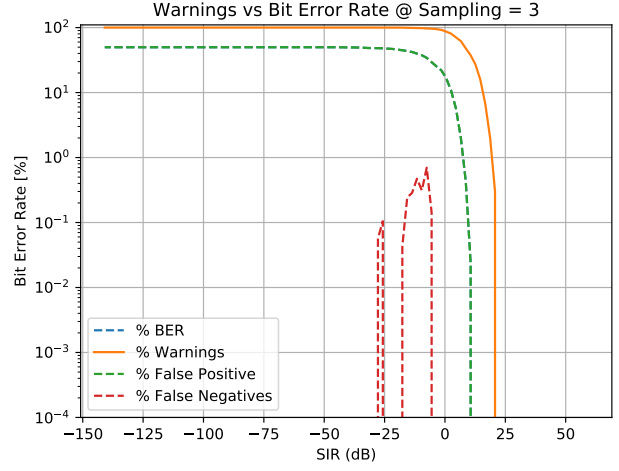


Fig. 8: Response of the EMI Detector for  $f_{\text{ratio}} = 3$  i.e.  $f_{\text{BIT}} = 166\text{MHz}$ ,  $f_{\text{EMI}} = 500\text{MHz}$ , distance between lines = 60mm

## VI. CONCLUSION

This paper analyses the performance of inverted-pair EMI detector using the Monte-Carlo based-simulation framework. The simulation framework is used to create a real-like reverberation environment; It can be concluded that the previously analysed theoretical results of proposed EMI detector are similar to the performance of EMI detector in a reverberation room environment. Inverted-pair EMI detector works quite effectively in comparison to a comparator based detector proposed in [7]. The performance of the proposed EMI detector has been analysed based on two main metrics; the number of false positives and the number of false negatives. EMI detector mainly focused on the lower false negatives. Results show, that the EMI detector can detect all disturbances when  $f_{\text{ratio}}$  is not multiple of samples per bit. On the other hand, when  $f_{\text{ratio}}$  is

multiple of samples per bit, EMI detector generates false negatives. The number of false negatives soars with the increase in distance between data transmission lines, increasing phase difference of EMI induced voltages in both data transmission lines. Overall, inverted-pair EMI detector can significantly enhance the safety of modern digital communication and allow the system to follow a precautionary procedure in case EMI disturbs the system. As this EMI detector is not able to remove false negatives for all cases, future work will focus on eliminating false negatives further and also on decreasing number of false positives.

## REFERENCES

- [1] J. Lannoo, A. Degraeve, D. Vanoost, J. Boydens, and D. Pisssoort, "Effectiveness of inversion diversity to cope with EMI within a two-channel redundant system," in *2018 IEEE International Symposium on Electromagnetic Compatibility and 2018 IEEE Asia-Pacific Symposium*

- on *Electromagnetic Compatibility, EMC/APEMC 2018*. Institute of Electrical and Electronics Engineers Inc., jun 2018, pp. 216–220.
- [2] J. Van Waes, J. Lannoo, J. Vankeirsbilck, A. Degraeve, J. Peuteman, D. Vanoost, D. Pissoort, and J. Boydens, “Effectiveness of hamming single error correction codes under harsh electromagnetic disturbances,” in *2018 International Symposium on Electromagnetic Compatibility (EMC EUROPE)*, Aug 2018, pp. 271–276.
- [3] J. Lannoo, A. Degraeve, D. Vanoost, J. Boydens, and D. Pissoort, “Study on the use of different transmission line termination strategies to obtain EMI-diverse redundant systems,” in *2018 IEEE International Symposium on Electromagnetic Compatibility and 2018 IEEE Asia-Pacific Symposium on Electromagnetic Compatibility (EMC/APEMC)*, May 2018, pp. 210–215.
- [4] J. Lannoo, J. V. Waes, D. Vanoost, J. Boydens, and D. Pissoort, “Analysis of availability and safety considerations in em-diverse systems,” in *2019 International Symposium on Electromagnetic Compatibility - EMC EUROPE*, 2019, pp. 927–932.
- [5] D. Pissoort, J. Lannoo, J. V. Waes, A. Degraeve, and J. Boydens, “Techniques and measures to achieve EMI resilience in mission- or safety-critical systems,” *IEEE Electromagnetic Compatibility Magazine*, vol. 6, no. 4, pp. 107–114, Fourth 2017.
- [6] F. Vanhee, D. Pissoort, J. Catrysse, G. A. E. Vandenbosch, and G. G. E. Gielen, “Efficient reciprocity-based algorithm to predict worst case induced disturbances on multiconductor transmission lines due to incoming plane waves,” *IEEE Transactions on Electromagnetic Compatibility*, vol. 55, no. 1, pp. 208–216, 2013.
- [7] J. Lannoo, A. Degraeve, D. Vanoost, J. Boydens, and D. Pissoort, “Effectiveness of inversion diversity to cope with EMI within a two-channel redundant system,” in *2018 IEEE International Symposium on Electromagnetic Compatibility and 2018 IEEE Asia-Pacific Symposium on Electromagnetic Compatibility (EMC/APEMC)*, May 2018, pp. 216–220.